New Journal of Physics
The open-access journal for physics

Collisional and molecular spectroscopy in an ultracold Bose–Bose mixture

G Thalhammer[1], G Barontini[1], J Catani[1,2], F Rabatti[1], C Weber[1,4], A Simoni[3], F Minardi[1,2,5] and M Inguscio[1,2]

[1] LENS European Laboratory for Nonlinear Spectroscopy and Università di Firenze, Via N Carrara 1, 50019 Sesto Fiorentino, Italy
[2] CNR-INFM, Via G Sansone 1, 50019 Sesto Fiorentino, Italy
[3] Laboratoire de Physique des Atomes, Lasers, Molécules et Surfaces, UMR 6627 du CNRS and Université de Rennes, 35042 Rennes Cedex, France
E-mail: minardi@lens.unifi.it

New Journal of Physics **11** (2009) 055044 (12pp)
Received 20 January 2009
Published 14 May 2009
Online at http://www.njp.org/
doi:10.1088/1367-2630/11/5/055044

Abstract. The route towards a Bose–Einstein condensate (BEC) of dipolar molecules requires the ability to efficiently associate dimers of different chemical species and transfer them to the stable rovibrational ground state. Here, we report on recent spectroscopic measurements of two weakly bound molecular levels and newly observed narrow d-wave Feshbach resonances. The data are used to improve the collisional model for the Bose–Bose mixture $^{41}K^{87}Rb$, one of the most promising candidates to create a molecular dipolar BEC.

[4] Present address: Institut für Angewandte Physik, Universität Bonn, Wegelerstrasse 8, D-53115 Bonn, Germany.
[5] Author to whom any correspondence should be addressed.

Contents

1. Introduction

A new tide in the domain of quantum degenerate gases is rising. Degenerate dipolar molecules, created from ultracold or degenerate atoms, are within reach. Such molecules will enable the study of zero-temperature systems with strong long-range interactions, whereas degenerate atoms interact substantially only through contact potentials. Degenerate molecules with dipole–dipole interactions will provide new quantum phases, will allow the simulation of magnetic spin systems and will provide candidate qubits for quantum computation.

Ultracold molecules have been produced by several groups, using either laser-cooled atoms in a magneto-optical trap (MOT) [1] or degenerate atoms [2]. Due to the energy–momentum conservation, molecular association cannot be a simple two-body process but requires a three-body collision, the exchange of photons (photoassociation) or adiabatic transitions (magnetoassociation).

Molecular Bose–Einstein condensates (BECs) have already been created [3, 4], but so far only with homonuclear dimers, whose electric dipole moment is necessarily zero. On the other hand, heteronuclear molecules have been created starting from ultracold but not degenerate samples [5]. A common challenge to all weakly bound dimer samples is relaxation decay. Whereas in a MOT the production of molecules directly in the rovibrational ground state has been demonstrated [6], the more efficient association from degenerate or quasi-degenerate ($T < 1\ \mu$K) atomic samples yields molecules in weakly bound state that are inevitably unstable to relaxation towards lower lying rovibrational levels. Only recently have ^{40}K^{87}Rb dimers, which were created by magnetoassociation, been transferred to the rovibrational ground state. Their electric dipole moment has been measured to be 0.566 Debye [7], in an experiment that represents a milestone in the route towards degenerate dipolar molecules.

The production of a BEC of dipolar molecules, however, requires the association of either two bosons or two fermions. Therefore we chose to investigate the Bose–Bose mixture ^{41}K^{87}Rb in which we associated the first double-species bosonic molecules [8]. Later, bosonic dimers were also created in a Fermi–Fermi mixture of ^{6}Li^{40}K [9]. For both association and state-transfer, an accurate knowledge of the interatomic potential is essential. In this paper, we report spectroscopic measurements on the ^{41}K^{87}Rb weakly bound levels, together with newly observed d-wave Feshbach resonances. We use this new set of data to improve the collisional model

for KRb [10], earlier adjusted to fit the extensive observations of Feshbach resonances in the isotopic ^{40}K^{87}Rb mixture [11, 12]. Accurate knowledge of the interatomic potential between ^{41}K and ^{87}Rb is essential for devising the transfer of molecules towards the low rovibrational states. The present work is therefore instrumental in the production of bosonic KRb molecules with long-range dipolar interactions.

The paper is organized as follows: in section 2, we describe our experimental procedure, and in section 3, we present the data. The theoretical results obtained by the adjustment of the collisional model are reported in section 4. Finally, we discuss the prospects for a KRb dipolar condensate.

2. Experimental set-up

Our experimental set-up consists of two separate two-dimensional MOTs, which deliver cold atomic beams of ^{41}K and ^{87}Rb [13] into a double-species three-dimensional MOT. The laser-cooled mixture is loaded in a quadrupole magnetic trap with a gradient of 260 G cm^{-1} that is subsequently translated by 31 mm with a motorized stage. The quadrupole magnetic field is converted into a harmonic magnetic trap generated by means of the millimetric trap described in [14]. Then we start the microwave evaporation that expels only ^{87}Rb atoms and cools the mixture (sympathetic cooling) down to approximately 2 μK. At this stage, the magnetic trap is replaced by a crossed dipole trap generated by two orthogonal laser beams at 1064 nm, with waists of $\sim$90 μm. Once the magnetic potential is completely extinguished, both species are transferred from the $|F = 2, m_F = 2\rangle$ to the $|1, 1\rangle$ hyperfine state, by means of consecutive radio-frequency (rf) ramps in the presence of a horizontal bias magnetic field of 7 G (adiabatic rapid passage). To guarantee the stability of the mixture against spin-changing collisions, it is important to transfer the species with the largest hyperfine splitting first and only later the second species: in our case, we transfer ^{87}Rb first and then ^{41}K. The adiabatic rapid passages last approximately 30 ms each and feature efficiencies ranging from 80 to 95%.

We raise a homogeneous magnetic field (the Feshbach field) along the vertical direction to access the interspecies Feshbach resonances. We calibrate the Feshbach field by measuring the frequency of ^{87}Rb hyperfine transitions. While the field resolution is 20 mG, reproducibility is limited to 50 mG.

The mixture is further cooled by lowering the power of the dipole trap beams to reach temperatures ranging from 300 to 600 nK with typically a few 10^4 atoms of each species. The mixture is now prepared for the subsequent experiments.

To associate the molecules and to measure the dimer binding energy, we modulate the Feshbach field with an additional excitation coil, driving transitions from unbound to bound pairs. The excitation frequencies range from 50 to 200 kHz, but we can drive the transitions also with half the resonant frequency, effectively doubling the range of the measurable binding energies. The excitation is 15–30 ms long, with a square amplitude envelope. As explained in [8], we determined our typical excitation amplitudes to be 130 mG.

The association of molecules is revealed by the loss of trapped atoms after the excitation pulse as we scan the excitation frequency. Such losses, resonant with the excitation frequency, occur when unbound pairs are converted into weakly bound dimers. Indeed these dimers are lost from the trap as soon as the subsequent inelastic collisions rapidly drive them into more deeply bound levels with a kinetic energy larger than the trap depth.

Likewise, the detection of the Feshbach resonances is obtained by the atomic losses caused by three-body recombination collisions. We therefore measure the number of atoms remaining after a fixed time in the dipole trap (hold time) as we scan the Feshbach field [15]. This method is especially useful for narrow resonances (such as those of higher partial waves), while it is poorly accurate in the case of broad Feshbach resonances, since the complex dynamics of atoms and weakly bound dimers must be taken into account to determine the exact position of Feshbach resonance from the inelastic losses. When possible, the positions of Feshbach resonances are better determined from extrapolation to zero of the measured binding energies.

3. Experimental results

We report here two different results, which are both important for improving the accuracy of the collisional model for $^{41}K^{87}Rb$, namely the measurement of the binding energies of the s-wave Feshbach dimers and the detection of two narrow d-wave Feshbach resonances.

3.1. s-wave molecular levels

In the vicinity of Feshbach resonances, the binding energy of the shallowest molecular levels can be accurately measured using rf spectroscopy. Unbound atom pairs are associated into weakly bound dimers by means of an oscillating magnetic field $\mathbf{b}\cos(\omega t)$. In our experiment, the $\mathbf{b}$ field is parallel to the Feshbach field; therefore it represents a modulation of the latter [16]. The association occurs resonantly when the oscillation frequency matches the energy difference between the unbound pair, $E = E_{\mathrm{kin}}$, and the molecular level, $E = -E_{\mathrm{b}}$.

The associated dimers undergo inelastic collisions with the unbound atoms and decay to more deeply bound levels ('relaxation collisions'). In this process the binding energy is converted into kinetic energy that is shared by the collisional partners, which are both expelled from the trap. Thus, association of molecules can be detected as a resonant loss of the atomic sample, even if the molecules themselves are too short lived to be directly detected.

In [8] we reported the first creation of heteronuclear bosonic molecules by means of rf association. We measured the binding energies of the Feshbach molecular levels next to the Feshbach resonances at 38 and 79 G. The atomic losses display a line shape, shown in figure 1, that must be modelled to accurately extract the binding energy. For this purpose, we employ a simple model, which is described in the appendix, that captures the salient features of the line shape. Our analysis reveals that the line shape is inhomogeneously broadened due to the thermal distribution of kinetic energies of the unbound atoms. The uncertainty of the measured resonant frequencies is 1%, which is mainly due to the fit precision.

In the following, we use these data to improve on the collisional model, which predicts the weakly bound molecular levels near the scattering threshold and the scattering length as a function of the magnetic field.

3.2. Higher order Feshbach resonances

In addition to the strong losses caused by two s-wave Feshbach resonances, at 38 and 79 G, respectively, we observe two narrow features, which we attribute to higher partial wave Feshbach resonances based on the collisional model developed in [10]. These peaks, shown

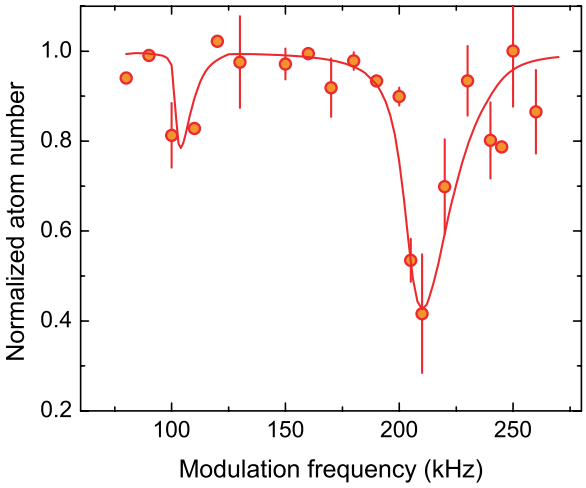

Figure 1. Line shape of rf association of Feshbach dimers around the Feshbach resonance at 79 G: we show the data on the normalized total atom number $N_K + N_{Rb}$ remaining after the 15 ms long rf pulse (solid circles), together with the result of numerical integration of the model described in the appendix (line). We also observe molecular association at half the resonance frequency.

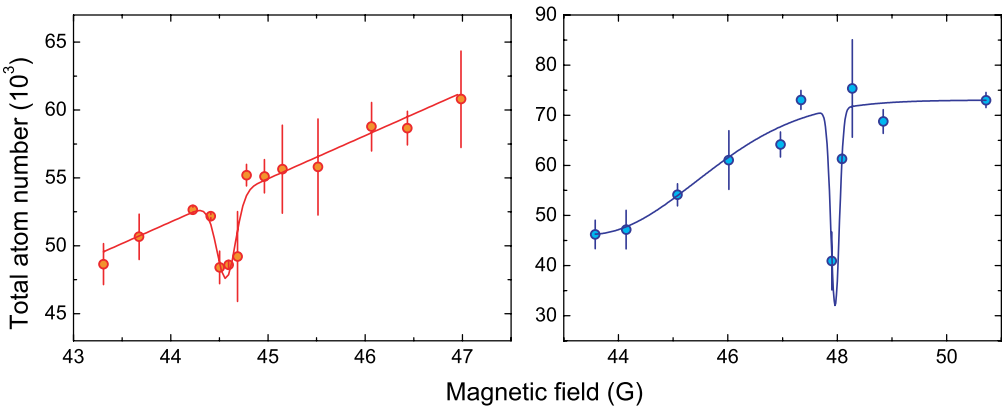

Figure 2. Loss features corresponding to the narrow d-wave Feshbach resonances. Both features are fitted by a narrow Gaussian line shape on a broader pedestal, that is linear in (a) and Gaussian in (b). Notice that the data set (b) does not show the feature at 44.6 G since the magnetic field steps are too coarse around this value.

in figure 2, were observed by simply holding the atomic mixture in the optical trap for 100 ms at different magnetic fields.

A first loss feature, detected at a temperature of 400 nK, is centred at a magnetic field of 44.58(0.05) G, with a very narrow half-width at half-maximum (HWHM) of 0.1 G.

The second loss feature is detected at a temperature of 450 nK, centred at a magnetic field of 47.96(0.02) G. The width of this peak, HWHM = 0.08 G, is at the limit of our experimental resolution. For both loss peaks the uncertainty of the position is mainly systematic and equals 0.05 G. The assignment of these narrow loss features to d-wave Feshbach resonances follows from the collisional model, as described in the next section.

Table 1. Comparison of experimental B_{exp} and theoretical B_{th} Feshbach resonance positions for collisions of ^{41}K and ^{87}Rb in their respective lowest Zeeman sublevel $|F = 1, m_F = 1\rangle$. Errors in theoretical data have been recalculated from the model. The molecular quantum numbers $(f m_f \ell')$ associated with the observed resonances are reported in the rightmost column.

B_{exp} (G)	B_{th} (G)	Assignment
44.58(5)	44.63(2)	(212)
47.96(10)	47.90(6)	(202)
78.57(5)	78.67(4)	(320)

Table 2. Comparison of observed $E_{\mathrm{m,\,exp}}$ and numerically calculated $E_{\mathrm{m,th}}$ s-wave molecular levels as a function of the magnetic field B. The rightmost column shows the molecular quantum numbers $(f m_f \ell')$. Errors in the $E_{\mathrm{m,\,exp}}$ column have been used for the weighted χ^2 and account for direct energy error plus the uncertainty 0.05 G in the magnetic field (see text). Errors in theoretical data have been recalculated from the model.

B (G)	$E_{\mathrm{m,\,exp}}$ (kHz)	$E_{\mathrm{m,th}}$ (kHz)	$(f m_f \ell')$
14.62	−142(2)	−141.0(9)	(220)
16.20	−128(2)	−130.7(8)	
16.25	−132(2)	−130.3(8)	
16.80	−130(2)	−126.6(8)	
17.82	−118(2)	−119.6(8)	
19.50	−107(2)	−107.7(7)	
77.83	−454(25)	−400(16)	(320)
77.92	−344(25)	−321(14)	
78.01	−264(15)	−250(13)	
78.10	−194(15)	−187(12)	
78.19	−134(15)	−132(11)	
78.24	−114(15)	−107(10)	
78.25	−114(15)	−102(10)	
78.35	−65(15)	−58(9)	

4. Theoretical results

The collisional properties of KRb isotopes are well understood. In [10], the data on ^{39}K^{87}Rb and ^{40}K^{87}Rb Feshbach resonances have been used to construct an accurate quantum scattering model. Here, we add to the data set binding energies as a function of the magnetic field of two near dissociation levels and magnetic resonance positions in the ^{41}K^{87}Rb isotopic pair (see tables 1 and 2). Molecular state energies are particularly valuable as they are immune to possible systematic shifts affecting the determination of the two-body resonance locations obtained from the observed maxima of the three-body recombination rate.

Our numerical calculations use the collision model built in [10]. The short-range molecular potentials are parameterized in terms of singlet and triplet s-wave scattering lengths, a_{s} and a_{t}.

The long range interatomic interaction is expanded in a multipole series in terms of C_6, C_8 and C_{10} dispersion coefficients. Relativistic interactions are relatively weak for alkali species. Inclusion of the dipolar interaction between the atomic electron spins and inclusion of the second-order spin–orbit interaction [17] are indeed sufficient to explain the available data on the isotopic pairs.

Here, we vary the singlet and triplet s-wave scattering lengths and the van der Waals coefficient C_6 until good agreement with the data is found. The additional potential parameters are fixed at the values of [10]. The energy levels included in the data are known to be molecular states with null orbital angular momentum ℓ'. The magnetic field location at which these levels become degenerate with the energy of the separated atoms corresponds to the two s-wave resonances observed in [15].

Note that in our fitting minimization procedure, the magnetic field is the independent variable and it is assumed as without error. The actual experimental uncertainty of B is accounted for by projecting it on the energy axis and adding it in quadrature to the direct measurement. As can be remarked from the data, the level corresponding to the 79 G resonance varies rapidly with magnetic field, such that a small B uncertainty of 0.05 G amounts to a $\sim$15 kHz error in the molecular state energy. Conversely, the level associated with the 38 G resonance varies more slowly with B and the error is determined by the direct energy measurement only.

We include in the data set two newly observed narrow features and the narrow s-wave resonance of [8], whose position can be very precisely determined. Magnetic resonances of different nature have been observed in cold atom collisions in a number of homonuclear [18] and heteronuclear systems [11, 19]. In general, broad resonances result from spin-exchange coupling of the incoming s-wave atomic pair with $\ell' = 0$ molecules. Such processes are induced by the spherically symmetric exchange interaction and conserve the orbital angular momentum ℓ, its projection m and the projection m_f of the total hyperfine spin of the system in the direction of the applied magnetic field.

Relativistic spin–spin and second-order spin–orbit interactions are anisotropic and enable first-order coupling of ℓ-wave atomic pairs with ℓ' symmetry molecules, provided that $|\ell' - \ell| \leqslant 2$, the $\ell = 0 \rightarrow \ell' = 0$ transitions being forbidden. Rotational symmetry about the external magnetic field implies exact conservation of the total angular momentum projection $m + m_f$. The total interaction couples incoming s-wave atomic pairs with $m_f = 2$ to states characterized by $\ell' = 0, 2$ and $0 \leqslant m_f \leqslant 4$. Higher order couplings to different ℓ' and m_f are possible but only give rise to much narrower features.

Collisions for atoms incoming in $\ell > 0$ partial waves tend to be suppressed at temperatures below the ℓ-wave centrifugal barrier. We take into account spin-exchange p-wave resonances, characterized by $\ell' = 1$ and $m_f = 2$. Such resonances have been observed even at very low temperature [20]. Finally, p-wave resonances induced by spin–spin coupling are in principle possible but they can be expected to be even weaker because of the weak coupling strength and the energy suppression. The corresponding m_f for direct coupling with incoming p-waves is bounded to $0 \leqslant m_f \leqslant 4$.

The model of [10] allows us to give a tentative assignment of the data. To this aim, it is instructive to calculate the near-threshold molecular levels for the lowest values of orbital angular momentum $\ell' = 0, 1, 2$ (see figure 3). A simplified approach that neglects the spin interactions is fully adequate for this purpose, since the resulting level shifts are small. In this approximation m_f, ℓ and m are good quantum numbers. The f quantum number is precisely

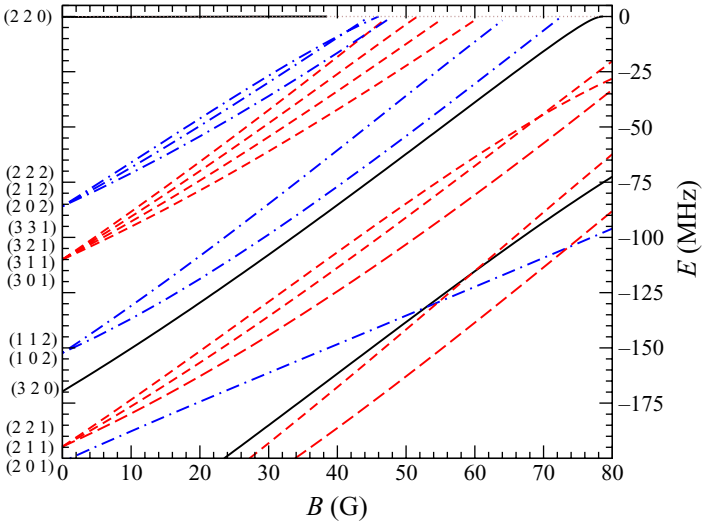

Figure 3. Molecular level scheme of $^{41}K^{87}Rb$ with $m_f = 0$–4 and $\ell' = 0$ (full line), 1 (dashed line), 2 (dash-dotted line). The quantum numbers $(f m_f \ell')$ are also shown. All energies refer to the atomic threshold, i.e. the energy of a pair of unbound atoms far apart.

defined only when $B = 0$. Thus, we use it as an approximate quantum label for the levels in the low-field domain $B < 80$ G of figure 3. We only show levels coupled in first order to incoming s- or p-wave atoms.

Figure 3 allows us to identify the molecular levels associated with the two observed loss features of figure 2. The one at lower field is univocally associated with a $\ell' = 2$ molecular level. The only possible ambiguity for the higher field feature arises from the crossing of a $\ell' = 1$ level with $m_f = 3$ very close to the observed value. This possibility is excluded since this feature would be a spin–spin-induced p-wave resonance. If such a weak feature were observable, one should then also observe a stronger spin-exchange p-wave loss feature at approximately 50 G, which is not detected. Moreover, with the present resolution one should observe the typical doublet structure of p-wave peaks [21]. We conclude that the molecular level associated with the 47 G resonance has also $\ell' = 2$ angular momentum.

With this assignment, we optimize our collisional model to obtain the best-fit parameters:

$$\begin{aligned} a_s &= -109(2)a_0, \\ a_t &= -213(3)a_0, \\ C_6 &= 4285(8)E_h a_0^6, \end{aligned} \tag{1}$$

where a_0 denotes the Bohr radius and E_h the Hartree energy.

The reduced weighted χ^2 is 0.92 and the maximum deviation between theoretical and empirical values is about two standard deviations. The present values are in agreement with [10]. In fact, if the bound states and the resonances in the three isotopic pairs are simultaneously fit, the following model potential parameters are determined:

$$\begin{aligned} a_s &= -109.6(2)a_0, \\ a_t &= -213.6(4)a_0, \end{aligned}$$

$$C_6 = 4288(2)\,E_h a_0^6, \qquad (2)$$
$$C_8 = 4.76(5) \times 10^5\,E_h a_0^8,$$
$$A_{ex} = 2.01(4) \times 10^{-3}\,E_h.$$

At variance with [10] the strength A_{ex} of the exchange interaction [22] is also included in the fit parameters. The quality of the fit is similar to the one of [10] with a reduced χ^2 of 1.1 and a maximum discrepancy with the experimental data of at most two standard deviations. The theoretical data do not show any systematic positive or negative shift with respect to the observed features. This strengthens the conclusion obtained in [10] that breakdown of the Born–Oppenheimer approximation [23] does not produce measurable effects at the current level of precision.

5. Conclusions

We have shown that recently published data on rf association of Feshbach dimers and newly determined Feshbach resonances in higher order partial waves have led to an improved collisional model for $^{41}K^{87}Rb$. Such a collisional model is important for future experiments on this mixture. In particular, KRb dimers appear to be among the best candidates to produce a molecular BEC with dipolar interactions. Indeed, bosonic KRb should be amenable to efficient transfer towards the rovibrational ground state with a single Raman pulse, following the pioneering demonstration in their fermionic $^{40}K^{87}Rb$ counterparts [7]. The route to stable bosonic molecules presumably will take advantage of dimer association starting from atoms trapped in optical lattices. As already recognized in [24], a double Mott insulator with unit filling (per species) will enable the creation of molecules secluded in individual lattice sites, thereby shielded from collisions with both unbound atoms and other molecules [25]. In addition, the lattice is an essential tool for implementing several models of bosons with long range interactions [26].

Acknowledgments

We acknowledge L De Sarlo and G Varoquaux for their contribution to the early stage of the experiment and all the members of the Quantum Degenerate Gases group in Florence for discussions. The CNR (EuroQUAM DQS, QUDIPMOL), Ente Cassa di Risparmio di Firenze, EU (STREP CHIMONO, NAMEQUAM) and INFN (SQUATSuper) are acknowledged for financial support.

Appendix

We describe here the theoretical model we used to fit the line shape of the rf association spectrum, i.e. of the total atom number remaining after an rf pulse of fixed length as a function of the rf frequency. Despite several simplifying approximations, the model captures the main features of the process, such as the broadening and the asymmetry of the spectrum. It is worth mentioning that the very same model was summarily described and applied in the analysis of [8]. Here we report a more detailed derivation of the line shapes.

We consider an atom pair in the center-of-mass reference frame. We introduce the annihilation operators for atoms A with momentum p, atoms B with momentum $-p$ and dimers with zero momentum: $\hat{a}$, $\hat{b}$ and $\hat{m}$. In the absence of rf coupling, the time-dependent free Hamiltonian is $\hat{H}_0 = (-E_{\rm bind}(B(t)) - {\rm i}\gamma/2)\hat{m}^\dagger\hat{m} + p^2/(2m_{\rm A})\hat{a}^\dagger\hat{a} + p^2/(2m_{\rm B})\hat{b}^\dagger\hat{b}$, where $m_{\rm A}$ and $m_{\rm B}$ denote the atomic masses and the time-dependence of the binding energy is brought by the dependence of the (positive-defined) binding energy $E_{\rm bind}$ on the oscillating Feshbach field $B(t) = B_{\rm dc} + b\sin(\omega t)$. The molecules have a finite lifetime γ^{-1}, due to relaxation processes.

The coupling is due to the oscillating part of the Feshbach field. Following [27], we consider a single-particle coupling strength proportional to the derivative of the oscillating field $\Omega(B(t)) = \Omega_0(B_{\rm dc})\cos(\omega t)$, with $\Omega_0(B) := \omega b(\frac{\partial}{\partial B'}\langle\psi_m(B)|\psi(B')\rangle)_{B'=B}$. Thus the rf coupling Hamiltonian is given by $\hat{H}_{\rm rf} = \Omega(t)(\hat{m}^\dagger\hat{a}\hat{b} + \hat{a}^\dagger\hat{b}^\dagger\hat{m})$. With this, we write the Heisenberg equation for the operators $\hat{a}, \hat{b}, \hat{m}$ and take the expectation values while neglecting all correlations. In practice, we replace the above operators with c-numbers α, β, μ:

$$\begin{aligned} {\rm i}\dot{\mu} &= (-E_{\rm bind}(t)/\hbar - {\rm i}\gamma/2)\,\mu + \Omega_0\cos(\omega t)\alpha\beta, \\ {\rm i}\dot{\alpha} &= p^2/(2\hbar m_{\rm A})\,\alpha + \Omega_0\cos(\omega t)\beta^*\mu, \\ {\rm i}\dot{\beta} &= p^2/(2\hbar m_{\rm B})\,\beta + \Omega_0\cos(\omega t)\alpha^*\mu. \end{aligned} \tag{3}$$

As expected from the conservation of total number of particles, the quantity $2|\mu|^2 + |\alpha|^2 + |\beta|^2$ is constant for $\gamma = 0$.

We can solve analytically this set of nonlinear Bloch equations, provided we introduce (i) the rotating-wave approximation, i.e. we write the equations in terms of the slowly varying amplitudes $\tilde{\alpha} := \alpha\exp({\rm i}p^2/(2\hbar m_{\rm A})t)$, $\tilde{\beta} := \beta\exp({\rm i}p^2/(2\hbar m_{\rm B})t)$, $\tilde{\mu} := \mu\exp(-{\rm i}(\omega - E_{\rm kin}/\hbar)t)$, with $E_{\rm kin} = p^2/(2m_{\rm A}) + p^2/(2m_{\rm B})$, and neglect all rapidly oscillating terms; (ii) the adiabatic approximation, whereby we consider that, since the molecular decay rate is fast, we can take the molecular amplitude $\tilde{\mu}$ to adiabatically follow the evolution dictated by the slower rf coupling, in practice ${\rm d}\tilde{\mu}/{\rm d}t = 0$. As a consequence, we have:

$$\begin{aligned} \tilde{\mu} &= -\frac{\Omega_0}{2(\delta - {\rm i}\gamma/2)}\tilde{\alpha}\tilde{\beta}, \\ \dot{N}_{\rm A} &:= \dot{\alpha}\alpha^* + {\rm c.c.} = -\frac{\gamma\Omega_0^2}{4\delta^2 + \gamma^2}N_{\rm A}N_{\rm B}, \\ \dot{N}_{\rm B} &:= \dot{\beta}\beta^* + {\rm c.c.} = -\frac{\gamma\Omega_0^2}{4\delta^2 + \gamma^2}N_{\rm A}N_{\rm B} \end{aligned} \tag{4}$$

with $\delta := \omega - E_{\rm bind}/\hbar - E_{\rm kin}/\hbar$.

Obviously the difference $n := N_{\rm A} - N_{\rm B}$ remains constant, while the sum $N_{\rm tot} := N_{\rm A} + N_{\rm B}$ obeys the equation

$$\dot{N}_{\rm tot} = -\gamma_{\rm eff}(N_{\rm tot}^2 - n^2), \qquad \gamma_{\rm eff} := \gamma\frac{\Omega_0^2}{2(4\delta^2 + \gamma^2)} \tag{5}$$

that has the following solution:

$$N_{\rm tot}(t) = n\frac{C\exp(2n\gamma_{\rm eff}t) + 1}{C\exp(2n\gamma_{\rm eff}t) - 1}, \qquad C := \frac{N_{\rm tot}(0) + n}{N_{\rm tot}(0) - n}. \tag{6}$$

For $n = 0$, the above reduces to

$$N_{\rm tot}(t) = \frac{N_{\rm tot}(0)}{1 + N_{\rm tot}(0)\gamma_{\rm eff}t}, \tag{7}$$

which is the well-known solution of the rate equation $\dot{N} = -\gamma_{\rm eff}N^2$ that is used to describe losses due to two-body collisions.

The solution (6) depends on the atomic kinetic energy $E_{\rm kin}$, whose values are spread over a range of the order of the temperature T. Under our experimental conditions, the thermal distribution of kinetic energies dominates the broadening of the rf spectra over the linewidth dictated by the decay rate γ. In order to compare with the measured spectra, we need to take a thermal average of equation (6) by convolving with the Boltzmann distribution of kinetic energies proportional to $\sqrt{E_{\rm kin}}\exp(-E_{\rm kin}/k_{\rm B}T)$. The resulting line shape describes well the strong asymmetry of the observed spectra.

A more detailed inspection of equations (3) reveals another interesting feature: molecular association also occurs for fractional frequencies of the resonant frequency (see figure 1). This is experimentally observed and confirmed by the results of numerical integration of equations (3).

Indeed the fact that the binding energy is modulated at the rf frequency ω makes it possible that the molecular amplitude contains Fourier components oscillating at integer multiples of ω. When one of these harmonics is close to the time-averaged value of the binding energy, the transfer of population to the molecular level occurs.

Another important experimental finding confirmed by the numerical simulations is the shift of the resonant peak frequency occurring when the binding energy depends nonlinearly on the magnetic field detuning from the Feshbach resonance. This is also easily understood when we consider that the time-averaged binding energy is shifted from the value in the absence of modulation. If the binding energy is quadratic with the magnetic field detuning $E_{\rm bind} = \eta\Delta B^2$, which is the case next to a Feshbach resonance, we have that $\langle E_{\rm bind}\rangle_t = E_{\rm bind}(\Delta B_{\rm dc}) + \eta b^2/2$, since $\Delta B(t) = \Delta B_{\rm dc} + b\sin(\omega t)$. This relationship has been experimentally verified [8].

References

[1] Vanhaecke N, de Souza Melo W, Tolra B L, Comparat D and Pillet P 2002 *Phys. Rev. Lett.* **89** 063001

[2] Wynar R, Freeland R S, Han D J, Ryu C and Heinzen D J 2002 *Science* **287** 1016

[3] Jochim S, Bartenstein M, Altmeyer A, Hendl G, Riedl S, Chin C, Hecker Denschlag J and Grimm R 2003 *Science* **302** 2101

[4] Greiner M, Regal C A and Jin D S 2003 *Nature* **426** 537

[5] Ospelkaus C, Ospelkaus S, Humbert L, Ernst P, Sengstock K and Bongs K 2006 *Phys. Rev. Lett.* **97** 120402

[6] Mancini M W, Telles G D, Caires A R L, Bagnato V S and Marcassa L G 2004 *Phys. Rev. Lett.* **92** 133203

[7] Ni K-K, Ospelkaus S, de Miranda M H G, Pe'er A, Neyenhuis B, Zirbel J J, Kotochigova S, Julienne P S, Jin D S and Ye J 2008 *Science* **322** 231

[8] Weber C, Barontini G, Catani J, Thalhammer G, Inguscio M and Minardi F 2008 *Phys. Rev.* A **78** 061601

[9] Voigt A-C, Taglieber M, Costa L, Aoki T, Wieser W, Hänsch T W and Dieckmann K 2009 *Phys. Rev. Lett.* **102** 020405

[10] Simoni A, Zaccanti M, D'Errico C, Fattori M, Roati G, Inguscio M and Modugno G 2008 *Phys. Rev.* A **77** 052705

[11] Ferlaino F, D'Errico C, Roati G, Zaccanti M, Inguscio M, Modugno G and Simoni A 2006 *Phys. Rev.* A **73** 040702

[12] Klempt C, Henninger T, Topic O, Will J, Ertmer W, Tiemann E and Arlt J 2007 *Phys. Rev.* A **76** 020701
[13] Catani J, De Sarlo L, Maioli P, Minardi F and Inguscio M 2006 *Phys. Rev.* A **73** 033415
[14] De Sarlo L, Maioli P, Barontini G, Catani J, Minardi F and Inguscio M 2007 *Phys. Rev.* A **75** 022715
[15] Thalhammer G, Barontini G, De Sarlo L, Catani J, Minardi F and Inguscio M 2008 *Phys. Rev. Lett.* **100** 210402
[16] Thompson S T, Hodby E and Wieman C E 2005 *Phys. Rev. Lett.* **95** 190404
[17] Mies F H, Williams C J and Julienne P S 1996 *J. Res. Natl Inst. Stand. Technol.* **101** 521
[18] Leo P J, Williams C J and Julienne P S 2000 *Phys. Rev. Lett.* **85** 2721
van Kempen E G M, Kokkelmans S J J M F, Heinzen D J and Verhaar B J 2002 *Phys. Rev. Lett.* **88** 093201
D'Errico C, Zaccanti M, Fattori M, Roati G, Inguscio M, Modugno G and Simoni A 2007 *New J. Phys.* **9** 223
[19] Burke J P, Bohn J L, Esry B D and Greene C H 1998 *Phys. Rev. Lett.* **80** 2097
Gacesa M, Pellegrini P and Côté R 2008 *Phys. Rev.* A **78** 010701
Wille E *et al* 2008 *Phys. Rev. Lett.* **100** 053201
[20] Schunck C H, Zwierlein M W, Stan C A, Raupach S M F, Ketterle W, Simoni A, Tiesinga E, Williams C J and Julienne P S 2005 *Phys. Rev.* A **71** 045601
[21] Ticknor C, Regal A C, Jin D S and Bohn J L 2004 *Phys. Rev.* A **69** 042712
[22] Zemke W T, Côté R and Stwalley W C 2005 *Phys. Rev.* A **71** 062706
[23] Falke S, Tiemann E and Lisdat C 2007 *Phys. Rev.* A **76** 012724
[24] Damski B, Santos L, Tiemann E, Lewenstein M, Kotochigova S, Julienne P and Zoller P 2003 *Phys. Rev. Lett.* **90** 110401
[25] Thalhammer G, Winkler K, Lang F, Schmid S, Grimm R and Hecker Denschlag J 2006 *Phys. Rev. Lett.* **96** 050402
[26] Góral K, Santos L and Lewenstein M 2002 *Phys. Rev. Lett.* **88** 170406
[27] Bertelsen J F and Mölmer K 2007 *Phys. Rev.* A **76** 043615